doi : 10.17596/0002545

白鳳丸研究航海報告

＊ 航海番号　　ＫＨ−２０−８次研究航海

＊ 航海名称　　海溝海側における海洋プレート上層部での流体循環と熱輸送過程の研究
および　相模トラフ巨大地震の震源断層に沿った流体湧出変動の研究
Study of pore fluid circulation and heat transport in the uppermost part of incoming plate on the seaward side of the trench,
Study on fluctuation of cold seep through a source fault of great earthquakes along the Sagami Trough

＊ 観測海域　　千島海溝・日本海溝・相模湾海域
Kuril Trench, Japan Trench and Sagami Bay areas

＊ 航海期間　　令和２年８月２４日（月）〜令和２年９月２日（水）

＊ 出港日時・場所　８月２４日１４時　八戸港

＊ 入港日時・場所　９月　２日１１時　東京港

＊ 寄港期間・場所　なし

＊ 研究課題　　海溝海側における海洋プレート上層部での流体循環と熱輸送過程の研究
相模トラフ巨大地震の震源断層に沿った流体湧出変動の研究

＊ 主席研究員（氏名・所属・職名）
山野　誠・東京大学地震研究所・教授

＊ 研究内容，主調査者，観測項目

１．地殻熱流量測定による、海洋地殻内の流体循環と熱輸送過程の研究
山野　誠、熱流量プローブ及びピストンコアラーによる熱流量測定

２．堆積物・間隙水試料採取による、断層近傍での流体流動の研究
鹿児島　渉悟、ピストンコアラー及びマルチプルコアラーによる堆積物および海底直上水の採取

３．海底電磁気観測による、太平洋プレート内の比抵抗構造の研究
　　後藤　忠徳、海底電位磁力計の回収

４．エアロゾル採取による、大気沈降物質の研究
　　張　勁、エアーサンプラーによるエアロゾル採取

５．堆積物試料採取による、断層活動の研究
　　芦　寿一郎、ピストンコアラー及びマルチプルコアラーによる堆積物採取

６．海底地形・地層探査による、地質構造の研究
　　芦　寿一郎、マルチビーム音響測深装置、地層探査装置（SBP）による地形・地質調査

７．海底長期温度計測による、湧水活動の研究
　　山野　誠、自己浮上式熱流量計の回収

＊ 乗船研究者氏名・所属・職名

山野　誠　・東京大学地震研究所・教授
木下　正高・東京大学地震研究所・教授
藤田　親亮・東京大学地震研究所・技術専門職員
芦　寿一郎・東京大学大気海洋研究所・准教授
亀尾　桂　・東京大学大気海洋研究所・技術専門職員
中西　諒　・東京大学大気海洋研究所・大学院生
後藤　忠徳・兵庫県立大学大学院生命理学研究科・教授
櫻井　未久・兵庫県立大学理学部・学部生
黒田真奈加・兵庫県立大学理学部・学部生
張　勁　　・富山大学学術研究部理学系・教授
鹿児島渉悟・富山大学学術研究部理学系・特命助教
野口　忠輝・富山大学大学院理工学教育部・大学院生
吉田　光佑・富山大学大学院理工学教育部・大学院生
大塚　進平・富山大学理学部・学部生
土岐　知弘・琉球大学理学部・准教授
満留　由来・琉球大学大学院理工学研究科・大学院生
笠谷　貴史・海洋研究開発機構海洋機能利用部門海底資源センター・グループリーダー
田中　明子・産業技術総合研究所活断層・火山研究部門・研究グループ長
宮嶋　優希・マリン・ワーク・ジャパン海洋地球科学部・観測技術員
小松　亮介・MOL マリン海洋事業室・観測技術員

＊ 測点・測線図

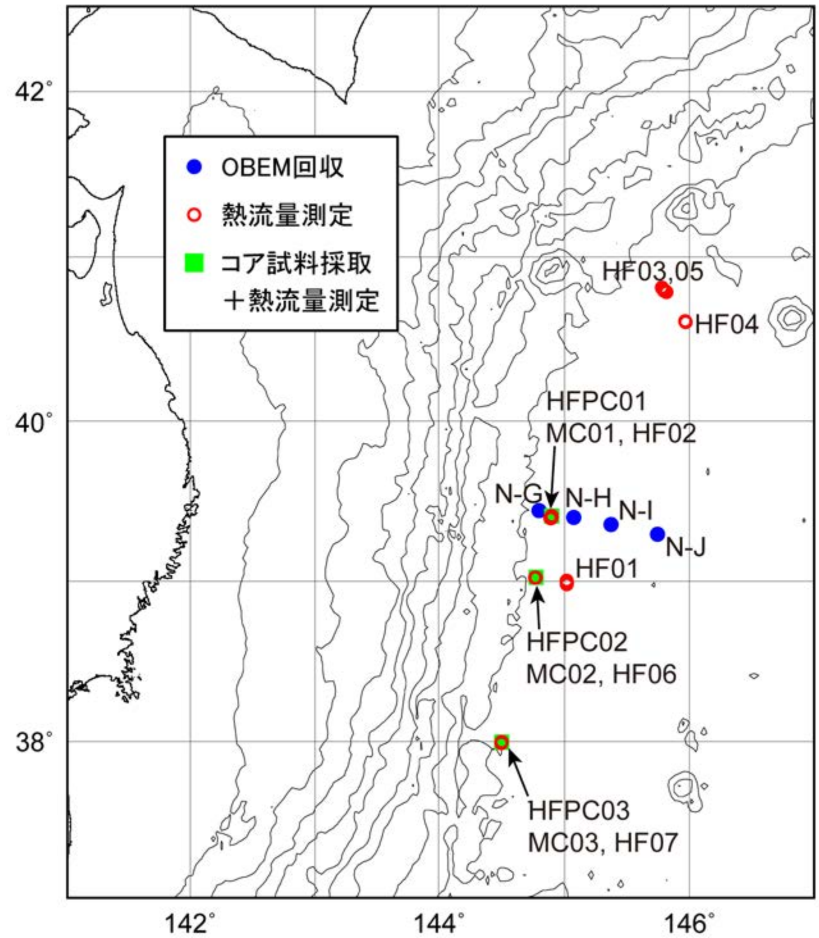
42°
40°
38°
142°
144°
146°
OBEM回収
熱流量測定
コア試料採取
＋熱流量測定
HF03,05
HF04
HFPC01
MC01, HF02
N-G
N-H
N-I
N-J
HF01
HFPC02
MC02, HF06
HFPC03
MC03, HF07

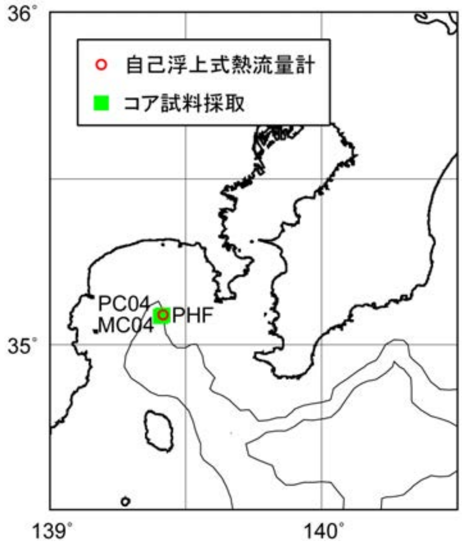
36°
35°
139°
140°
自己浮上式熱流量計
コア試料採取
PC04
MC04
PHF

Contents

1. Cruise Information

Cruise ID:

KH-20-8

Name of vessel:

R/V HAKUHO MARU

Title of cruise:

Study of pore fluid circulation and heat transport in the uppermost part of incoming plate on the seaward side of the trench

Study on fluctuation of cold seep through a source fault of great earthquakes along the Sagami Trough

Chief scientist:

Makoto YAMANO Earthquake Research Institute, The University of Tokyo

Cruise period:

August 24, 2020 – September 2, 2020

Ports of departure / arrival:

2020	August 24	Dept. from Hachinohe
	September 2	Arriv. at Tokyo

Research area:

Kuril Trench, Japan Trench and Sagami Bay areas

Research map:

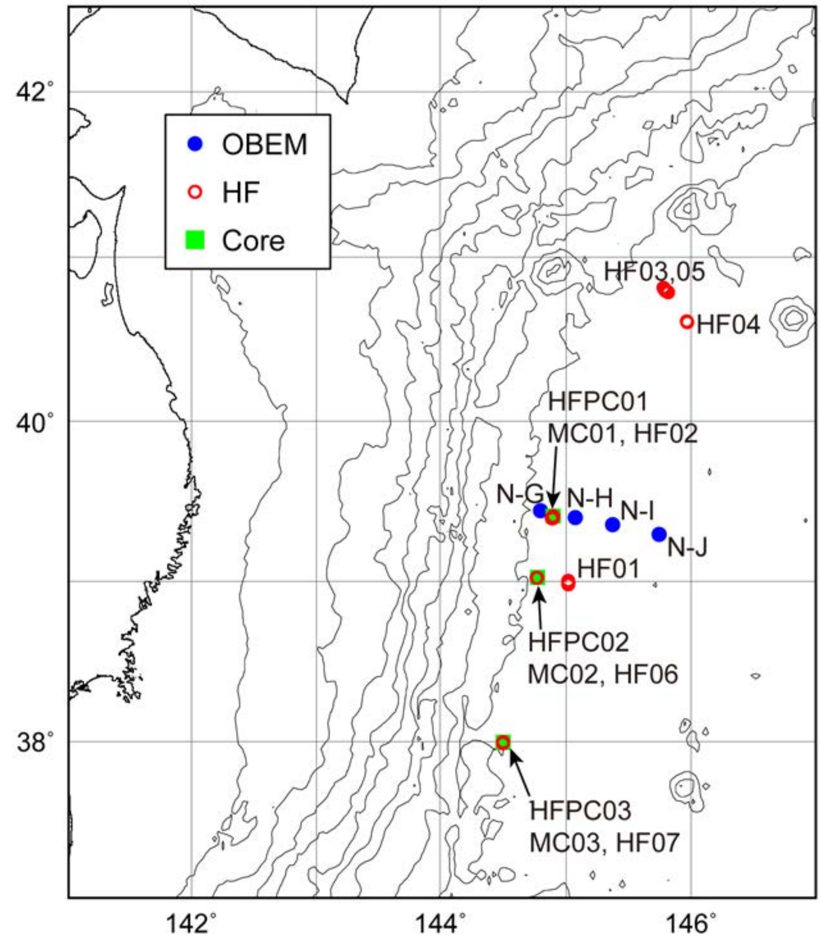

Figure 1-1. Locations of observation points in the Kuril and Japan trench areas. HF: heat flow measurement, Core: sediment sampling and heat flow measurement, OBEM: recovery of OBEM.

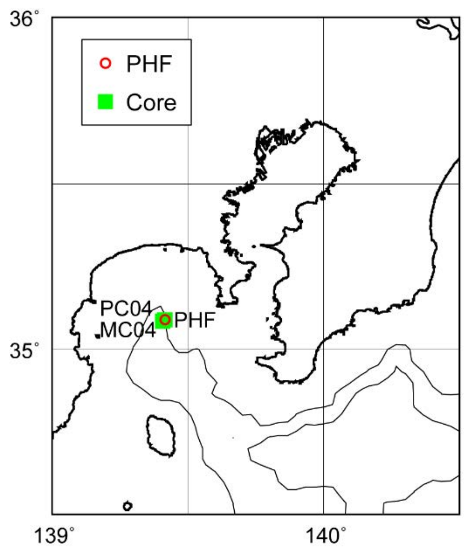

Figure 1-2. Locations of observation points in the Sagami Bay area. PHF: recovery of pop-up heat flow instrument (failed), Core: sediment sampling.

2. Research Proposal and Science Party

Title of proposal:

Study of pore fluid circulation and heat transport in the uppermost part of incoming plate on the seaward side of the trench

Study on fluctuation of cold seep through a source fault of great earthquakes along the Sagami Trough

Representative of science party:

Makoto YAMANO	Earthquake Research Institute, The University of Tokyo

Science Party:

Makoto YAMANO	Earthquake Research Institute, The University of Tokyo
Juichiro ASHI	Atmosphere and Ocean Research Institute, The University of Tokyo
Masataka KINOSHITA	Earthquake Research Institute, The University of Tokyo
Chikaaki FUJITA	Earthquake Research Institute, The University of Tokyo
Katsura KAMEO	Atmosphere and Ocean Research Institute, The University of Tokyo
Ryo NAKANISHI	Atmosphere and Ocean Research Institute, The University of Tokyo
Jing ZHANG	Faculty of Science, Academic Assembly, University of Toyama
Takanori KAGOSHIMA	Faculty of Science, Academic Assembly, University of Toyama
Tadateru NOGUCHI	Graduate School of Science and Engineering for Education, University of Toyama
Kosuke YOSHIDA	Graduate School of Science and Engineering for Education, University of Toyama
Shinpei OTSUKA	School of Science, University of Toyama
Tada-nori GOTO	Graduate School of Life Science, University of Hyogo
Miku SAKURAI	School of Science, University of Hyogo
Manaka KURODA	School of Science, University of Hyogo
Tomohiro TOKI	Faculty of Science, University of the Ryukyus
Yuki MITSUTOME	Graduate School of Engineering and Science, University of the Ryukyus
Takafumi KASAYA	Research Institute for Marine Resources Utilization, Japan Agency for Marine-Earth Science and Technology
Akiko TANAKA	Geological Survey of Japan, National Institute of Advanced Industrial Science and Technology
Kiyoshi BABA	Earthquake Research Institute, The University of Tokyo (shore-based)

Hiroshi ICHIHARA	Graduate School of Environmental Studies, Nagoya University (shore-based)
Kiichiro KAWAMURA	Graduate School of Sciences and Technology for Innovation, Yamaguchi University (shore-based)
Shusaku GOTO	Geological Survey of Japan, National Institute of Advanced Industrial Science and Technology (shore-based)
Hideki HAMAMOTO	Center for Environmental Science in Saitama (shore-based)
Gou FUJIE	Research Institute for Marine Geodynamics, Japan Agency for Marine-Earth Science and Technology (shore-based)
Yoshifumi KAWADA	Research Institute for Marine Resources Utilization, Japan Agency for Marine-Earth Science and Technology (shore-based)

Technical Support Staff

Yuki MIYAJIMA	Marine Works Japan, Ltd.
Ryosuke KOMATSU	MOL Marine Co., Ltd.

3. Research Activities

3.1. Research Objectives

Research activities on the KH-20-8 cruise are based on two independent proposals: (1) study of pore fluid circulation and heat transport in the uppermost part of incoming plate on the seaward side of the trench, (2) study on fluctuation of cold seep through a source fault of great earthquakes along the Sagami Trough.

In the first proposal, we aim to compare characteristics of heat flow distribution on the trench outer rise between the Kuril and Japan trenches, which may reflect pore fluid circulation and heat transport processes resulting from fracturing of the oceanic crust due to bending of the Pacific plate. We also investigate fluid flow along normal faults developed on the seaward slope of the Japan Trench through concentrated heat flow measurements and analysis of pore water and gas extracted from sediment samples. We recover ocean bottom electromagnetometers (OBEMs) deployed on the Japan Trench outer rise in 2019 and the obtained data will be used for estimation of the electrical resistivity structure related to pore fluid distribution.

The target of the second proposal is cold seep along faults on the landward slope of the Sagami Trough. We attempt to retrieve a long-term temperature recording instrument deployed in 2019 for monitoring fluid flow through sediment and take sediment core samples for study of depositional history.

3.2. Cruise Schedule and Operations

Date	Events, Operations
August 24	Leave Hachinohe Transit to the survey area (Kuril and Japan trench area)
August 25	Arrive in the survey area Recovery of three OBEMs (N-J, N-I, and N-H) Heat flow measurement (HF01)
August 26	Heat flow measurement (HF01, continued) Recovery of one OBEM (N-G) Bathymetry survey Heat flow measurement (HF02)
August 27	Heat flow measurement (HF02, continued) Core sampling (MC01) Core sampling with heat flow measurement (HFPC01) Heat flow measurement (HF03)
August 28	Heat flow measurement (HF03, continued) Heat flow measurement (HF04) Heat flow measurement (HF05)
August 29	Bathymetry survey Heat flow measurement (HF06) Core sampling with heat flow measurement (HFPC02) Core sampling (MC02)
August 30	Heat flow measurement (HF07) Core sampling with heat flow measurement (HFPC03) Core sampling (MC03) Transit to the 2nd survey area (Sagami Bay area)
August 31	Arrive in the 2nd survey area Core sampling (MC04)
September 1	Recovery of pop-up heat flow instrument (PHF, failed) Core sampling (PC04) Leave the 2nd survey area
September 2	Arrive at Tokyo

3.3. Research Activities

3.3.1. Heat flow measurement

1) Background and objectives

Anomalous heat flow values, higher than that expected for the seafloor age of the incoming Pacific plate, are pervasively distributed on the outer rise of the Japan Trench (Yamano et al., 2014). Overlapping the broad anomaly, local variations at a scale of several kilometers were detected through concentrated measurements along lines perpendicular to the trench. The broad high heat flow zone seaward of the trench can be attributed to pore fluid circulation in a permeable layer developed through fracturing of the oceanic crust due to plate bending, which efficiently pumps up heat from deeper part of the crust (Kawada et al., 2014). Local variations may have arisen from heterogeneous development of fractures: higher surface heat flow is observed at sites where the crust has been fractured down to deeper part.

On the seaward slope of the Japan Trench, where normal faults are well developed, heat flow data had been sparse compared to dense data on the outer rise. Preliminary measurements were made around faults with large surface displacement in 2015 and 2016 on the KS-15-16 and KS-16-15 cruises of the R/V SHINSEI MARU. On this cruise, we conduct more concentrated measurements in the vicinities of the 2015 and 2016 data for investigation of influence of normal faults on fluid flow and heat transport processes in the incoming oceanic crust.

We conducted heat flow measurements on the seaward side of the westernmost part of the Kuril Trench in 2018 on the KH-18-5 cruise of the R/V HAKUHO MARU. Heat flow on the Kuril Trench outer rise was found to be generally normal for the seafloor age, in contrast to the high anomaly off the Japan Trench. To examine this feature in more detail, additional measurements are made on this cruise along a line where the 2018 data were obtained.

2) Measurement method

Heat flow is obtained as the product of the geothermal gradient and the thermal conductivity. We measured the geothermal gradient by penetrating an ordinary deep-sea heat flow probe or a heat flow piston coring system (HFPC) into seafloor sediments.

[Instruments]

The deep-sea heat flow probe (Fig. 3.3-1) weighs about 800 kg and has a 3.0 m-long lance, along which seven compact temperature recorders (Miniaturized Temperature Data Logger, ANTARES Datensysteme GmbH; Fig. 3.3-2) are mounted in an outrigger fashion (Ewing type). A heat flow data logger (Kaiyo Denshi Co., DHF-650) placed inside the weight head (cf. Fig. 3.3-4) was used for recording the tilt and the depth of the probe. Tilt and depth data were sent to the surface with acoustic pulses so that we can monitor the status of the probe on the ship.

Temperature profiles in surface sediment were measured with a piston corer as well. For this purpose, we used a core head specially designed for mounting the heat flow data logger, and temperature recorders (MTLs) were attached along the 4-m long core barrel (Fig. 3.3-3). We call this system the heat flow piston coring system (HFPC). A 1-m long gravity corer with a liner tube of 75-mm diameter was used as the pilot corer.

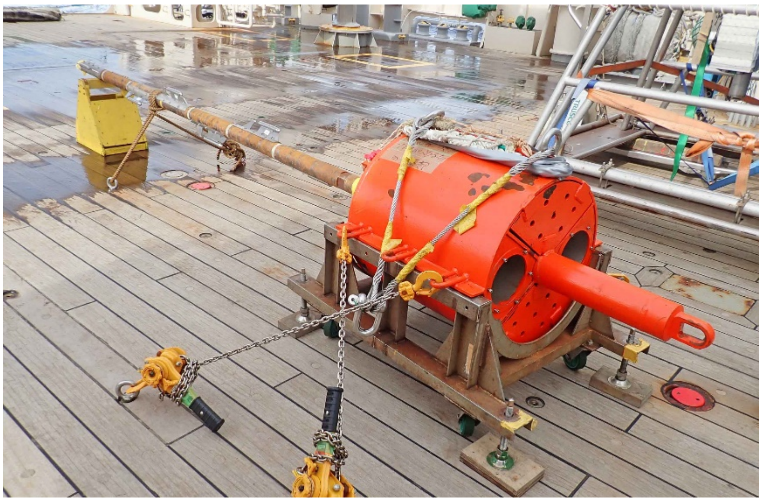

Figure 3.3-1. Deep-sea heat flow probe.

Figure 3.3-2. ANTARES Miniaturized Temperature Data Logger (MTL).

Figure 3.3-3. Heat flow piston coring system (HFPC) with temperature data loggers (MTLs).

[Operations]

A 20-m long nylon rope was inserted between the heat flow probe and the winch wire rope in order not to kink the wire rope during probe penetrations. An acoustic transponder was attached about 100 m above the probe for precise determination of the position of the probe (Fig. 3.3-4).

Multi-penetration heat-flow measurement operations were conducted following the procedures described below.

1. Measure water temperature about 30 m above the seafloor for calibration of the temperature recorders.
2. Lower the probe at a speed of about 1 m/sec until it penetrates into the sediment.
3. Measure temperatures in the sediment for about 15 min. Monitor the wire tension and pay out the wire when necessary to keep the probe stable.
4. Pull out the probe.
5. Move to the next station keeping the probe about 100 m above the seafloor.
6. Repeat penetrations.

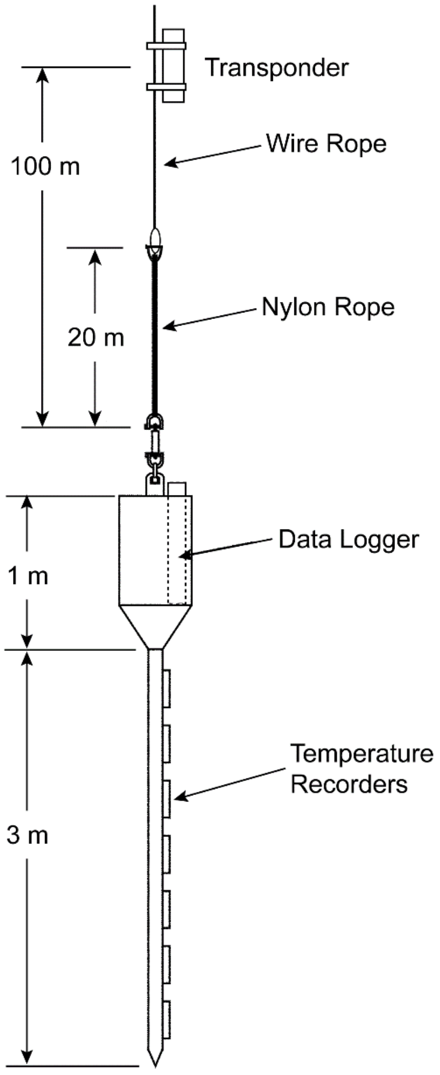

Figure 3.3-4. Configuration of the heat flow measurement system using a deep-sea probe.

The operation procedure for the HFPC is similar to that for ordinary piston coring system, except the HFPC is kept on the seafloor for about 15 min. for measurement of temperature distribution in sediment. The 20-m long nylon rope was used for the HFPC as well.

3) Preliminary results

We carried out heat flow measurements in three areas: 1) on the outer rise of the Kuril Trench around 41°N, 146°E, 2) in the vicinities of normal faults developed on the seaward slope of the Japan Trench, 3) along a short N-S line on the Japan Trench outer rise (around 39°00’N, 145°01’E) (cf. Fig. 1-1). Most of the measurements were made with the deep-sea heat flow probe at intervals of 300 to 400 m to detect local variations. At three core sampling sites (HFPC01, 02, and 03), the heat flow piston coring system (HFPC) was used.

We attempted 43 penetrations in total and 31 of them were successful (Table 3.3-1). Most of the coordinates of the measurement points in Table 3.3-1 are the positions of the acoustic transponder determined with the SSBL system of the ship. At some stations (HF01A to F, HF03, HF06, and HFPC03), the listed coordinates are the positions of the ship since the positions of the transponder were not well determined. The water depth in the table is the depth measured by the heat flow data logger, except the depths at HF04 and HFPC03, which are the depths right below the ship determined with the multi-beam echo-sounder and may be slightly different from the depths at the measurement points.

Heat flow measurements on the Kuril Trench outer rise were conducted at three sites (HF03, 04, and 05) on a line perpendicular to the trench axis. Measurements were made along the same line in 2018 as well and anomalously high values for the seafloor age were obtained at one site (KH-18-5 HF06). HF03 and 05 were located close to this high heat flow site to know the extent of the high anomaly.

Measurements in the vicinities of normal faults were made at three sites: HF02 and HFPC01 around 39.4°N, HF06 and HFPC02 around 39.0°N, HF07 and HFPC03 around 38.0°N. Two of them (HF02 and HFPC01, HF07 and HFPC03) are very close to sites where anomalously high $^{3}He/^{4}He$ ratios were found in pore water of surface sediment (Park et al., 2021, cf. 3.3.5.

On the Japan Trench outer rise around 39°N, previous concentrated survey along an E-W line normal to the trench showed prominent heat flow variations at a scale of 3 to 5 km. At HF01, we made measurements along a N-W line to examine heat flow variation in the trench-parallel direction.

Heat flow values will be obtained by combining the measured temperature profiles with thermal conductivity of surface sediment. Thermal conductivity needs to be estimated from the values measured on piston core samples and the existing data on the Japan and Kuril trench outer rises.

Table 3.3-1. Results of heat flow measurements

Date	Station	Latitude (N)	Longitude (E)	Depth (m)	N
Deep-sea heat flow probe					
Aug. 25	HF01A	38°59.51'*	145°01.03'*	5510	fell
	B	38°59.50'*	145°01.05'*	5510	fell
	C	38°59.50'*	145°01.06'*	5510	6
	D	38°59.82'*	145°01.05'*	5515	fell
	E	38°59.82'*	145°01.05'*	5515	7
Aug. 26	F	39°00.04'*	145°01.10'*	5520	6
	G	39°00.25'	145°01.08'	5525	6
	H	39°00.40'	145°01.00'	5530	7
	I	39°00.66'	145°01.00'	5535	4
	J	39°00.87'	145°00.98'	5535	4
	HF02A	39°24.97'	144°53.77'	5655	7
	B	39°24.75'	144°53.75'	5650	7
	C	39°24.44'	144°53.58'	5655	fell
	D	39°24.41'	144°53.57'	5655	fell
	E	39°24.41'	144°53.58'	5655	fell
	F	39°24.21'	144°53.56'	5655	7
Aug. 27	G	39°24.35'	144°53.00'	5625	7
	H	39°24.20'	144°53.21'	5660	7
	I	39°24.13'	144°53.30'	5660	5
	HF03A	40°49.28'*	145°46.83'*	5385	4
	B	40°49.03'*	145°47.05'*	5385	fell
	C	40°49.02'*	145°47.03'*	5385	4
Aug. 28	D	40°48.74'*	145°47.23'*	5380	4
	E	40°49.49'*	145°47.49'*	5380	5
	F	40°49.18'*	145°47.75'*	5385	fell
	G	40°49.18'*	145°47.76'*	5385	5
	HF04A	40°36.99'	145°57.97'	5190**	7
	B	40°36.88'	145°58.10	5180**	7
	C	40°36.70'	145°58.24'	5180**	7

		HF05A	40°47.85'	145°48.71'	5325	1
		B	40°47.76'	145°48.86'	5320	2
		C	40°47.64'	145°49.04'	5320	3
	Aug. 29	HF06A	39°01.98'*	144°46.10'*	5880	fell
		B	39°01.97'*	144°46.10'*	5880	fell
		C	39°01.97'*	144°46.09'*	5880	fell
		D	39°01.99'*	144°45.86'*	5875	4
		E	39°01.98'*	144°45.74'*	5875	6
	Aug. 30	HF07A	37°59.93'	144°29.70'	6015	5
		B	37°59.75'	144°29.64'	6020	7
		C	37°59.50'	144°29.52'	6035	7
HFPC						
	Aug. 27	HFPC01	39°24.97'	144°53.77'	5655	7
	Aug. 29	HFPC02	39°02.06'	144°46.29'	5880	3
	Aug. 30	HFPC03	37°59.91'*	144°29.67'*	6010**	5

N: number of temperature sensors used to obtain temperature profile in sediment.

*: position of the ship

**: water depth right below the ship

4) Thermal conductivity measurement

Thermal conductivity of sediment core samples was measured using two different types of line-source commercial devices. One is QTM-700 (Kyoto Electronics Manufacturing Co.) with a half-space type box probe (Sass et al., 1984). The other is KD2 Pro Thermal Properties Analyzer (Decagon Devices, Inc.) with a full-space type needle probe (von Herzen and Maxwell, 1959). KD2 Pro has the ability to measure thermal diffusivity (or heat capacity) as well as thermal conductivity by using dual-needle sensors (dual probes; Bristow et al., 1994), while measurements with ordinary single-needle sensors (single probes) give thermal conductivity only. We conducted measurements with these devices on split core samples.

3.3.2. Sediment core samples

Three core samples (HFPC01, HFPC03, PC04) were collected from the piston cores during the four operations (HFPC01, HFPC02, HFPC03, PC04). HFPC01 and HFPC03 are 280 and 210 cm long core samples collected in the B and C seas, respectively. HFPC02 was operated in area B, but no core samples were obtained. PC04 was sampled in area E, but is not described in this report because it was not cut in half. The following are the results of the descriptions of HFPC01 and HFPC03 in the field (Figs. 3.3-5 and 3.3-6).

HFPC01: The matrix of this core consists of dark olive silty mud. At a depth of 195 cm, a layer of gray volcanic ash with normal grading was observed. Several layers of fine-grain sand layers (ca. 2 cm) consisting of pumice were identified, including rework layers based on its patchy texture. Other features included scattered clasts (mm to 1 cm), glauconite dominant layers and black laminations.

HFPC03: The matrix of this core consists of dark olive silty mud. The entire hemipelagic mud included scattered clasts, mainly pumice (including chert rock). At a depth of 67 cm, a magnetic black silt layer including clasts was observed, and it had clear contacts above and below hemipelagic mud. Other features included glauconite dominant layers, dark green sandy mud and dark brown laminations.

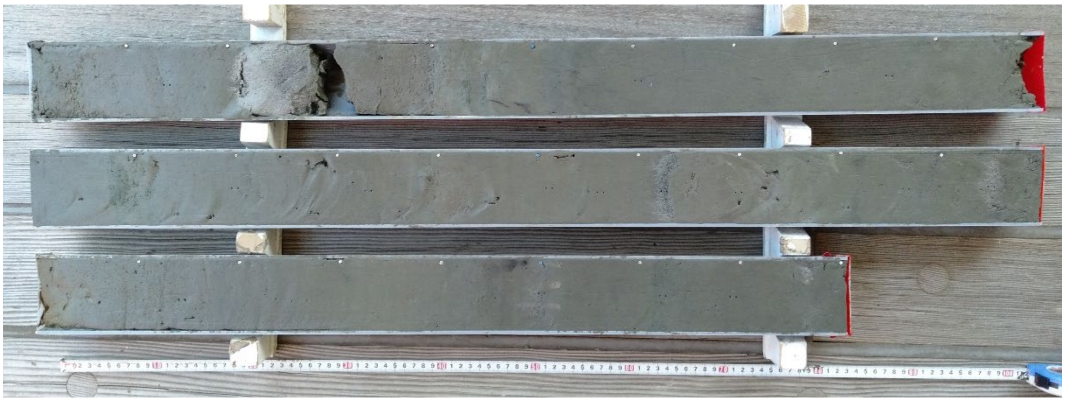

Figure 3.3-5. Photo of the HFPC01 core. From top to bottom, sections 4, 3 and 2, with the core top on the left.

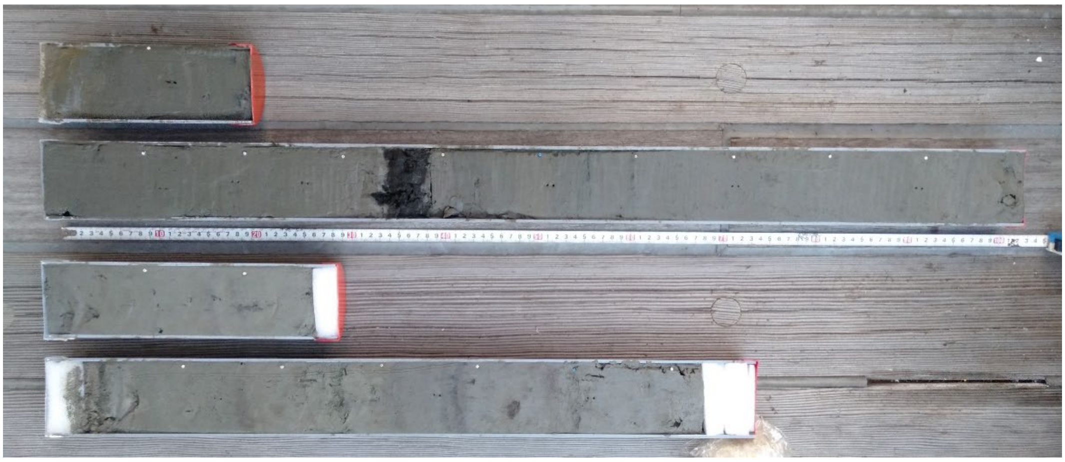

Figure 3.3-6. Photo of the HFPC03 core. From top to bottom, sections 1, 2, 3 and 4, with the core top on the left.

3.3.3. Interstitial water geochemistry (1) major elements

1) Background

It has been reported that a large slip occurred in the vicinity of the Japan Trench due to the earthquake happened in the Sanriku coastal area of Tohoku in 2011. However, little explanation of this phenomenon has been reported, and the shift on the ocean-side along the axis of the trench has not been quantified. In order to comprehend the heat and fluid distribution in the crust, it is important to understand the chemical composition of pore fluid based on heat flux and chemical analysis data.

In this study, sediment, overlying water and porewater were collected near the sea-side slope of the Japan Trench, to comprehend the pore fluid behavior, such as the heat transport and seawater inflow or outflow above the fault. Furthermore, the samples will be analyzed in terms of both microorganisms and chemical composition.

2) Sample collection

Sediment samples were collected using multiple, pilot and piston-corers. Based on the condition of the deposited layer and target parameters, the cores were sliced onboard, with intervals of 0.5 cm to 3 cm. Porewater was squeezed by using syringes under low temperature (ca. 4°C) onboard. The chemical composition and isotopes of porewater will be measured at onshore laboratories.

The sampling stations are shown below (Table 3.3-2). The Piston and Pilot-corer were used in HFPC01-HFPC04 and PC04 stations, and Multiple-corer was used in MC01-MC04 stations. No core samples were recovered at station HFPC02. In Fig. 3.3-7, the locations of these stations are shown on the map.

Table 3.3-2. Sediment sampling stations

Station	Latitude	Longitude	Depth	Date
HFPC01	39°24.97’ N	144°53.77’ E	5655m	2020/8/27 02:20 UTC
HFPC02	39°02.06’ N	144°46.29’ E	5880m	2020/8/29 07:46 UTC
HFPC03	37°59.91’ N	144°29.67’ E	6010m	2020/8/30 04:24 UTC
PC04	35°05.37’ N	139°24.88’ E	1105m	2020/8/31 23:34 UTC
MC01	39°24.99’ N	144°53.77’ E	5660m	2020/8/26 22:04 UTC
MC02	39°02.03’ N	144°46.34’ E	5875m	2020/8/29 12:15 UTC
MC03	37°59.86’ N	144°29.62’ E	6010m	2020/8/30 09:10 UTC
MC04	35°05.10’ N	139°24.35’ E	1145m	2020/8/31 12:35 UTC

3) Results and future plans

Gravel originated from land were found in sediments of MC01-MC03 stations. It was noted that muddy smell exists in the upward 30 cm of the MC04 sediment, where organisms were also observed. The silicate concentration in porewater were analyzed onboard, the results showed the concentration decreased at the depth of more than 1 m, so that the existence of advection can be inferred.

In the future, principal components and isotopes in porewater will be measured, and microbial communities will be identified. Combining these chemical analyses with physical observations, detailed compositions of pore fluid will be clarified. These results will be compared with those in previous cruises, especially KH-11-7 cruise.

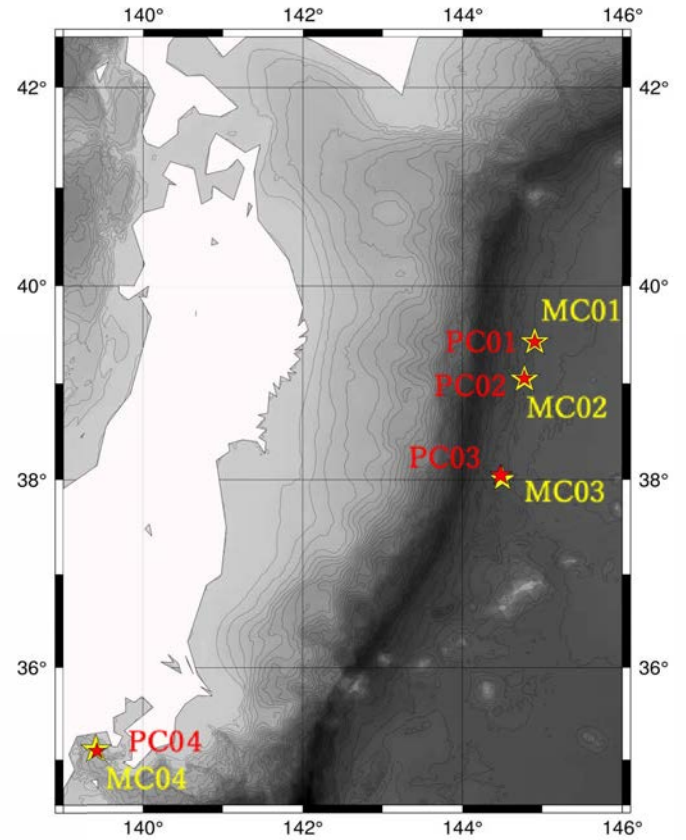

Figure 3.3-7. Location of Multiple-corer (MC) and Piston-corer (PC) stations in Sagami Bay and the coastal area of Sanriku.

3.3.4. Interstitial water geochemistry (2) minor elements

1) Introduction

In this area, seawater flows into the mantle through normal faults formed at the bend of the plate, and the faults connected to the mantle play also roles as supply channels for mantle-derived helium, so that high helium isotope ratios ($^{3}He/^{4}He$) have been found in surface sediments (Park et al., 2021).

Boron isotope ratios include ^{10}B and ^{11}B, and ^{10}B is adsorbed on the surface of sediments at subseafloor (Spivack et al., 1987). When the sediments are buried to deeper layers, and the ambient temperature becomes as high as ~200 °C, ^{10}B is incorporated into the lattice of clay minerals related to their dehydration (Williams et al., 2001). When sediments collected at about 1,000 m below the seafloor were boiled with seawater at high temperature in hydrolysis experiments, ^{10}B was released (You et al., 1996; You et al., 1995). Geothermometers using boron isotope ratios have been proposed, and when equilibrium is reached with the solid phase at higher temperatures, fluids with lower boron isotope ratios, close to those of solids, are formed (Deyhle and Kopf, 2005). Thus, if deep fluids are detected in the surface layer, then lower isotopic boron that has reached equilibrium with the solid at higher temperatures could be detected in the surface layer. Therefore, the purpose of this study is to collect surface sediments, extract pore water, measure trace element concentrations and boron isotope ratios in the samples, detect signs of deep fluid, and determine the origin depth of the fluid using a geothermometer.

2) Sampling

2-1) Piston corer

Sediments were recovered by piston corers, and the sampled sediments in the piston corers were cut every 1 m of section. The sediments in the sections were split in half, and ~5 cm^3 of sediment was collected from the interval listed in Table 3.3-3 using a 3-mL syringe (HENKE; luer tip all plastic syringe) for moisture content weighing and placed in a plastic bag with zipper. Similarly, 5 cm^3 of sediment for headspace gas analysis was collected and placed in a glass vial (Maruemu Corporation; 50 mL vial bottle), 1 mL of saturated mercuric dichloride solution was added, and the vial was capped with a rubber stopper and aluminum seal. Then, the sediment and saturated mercuric chloride solution in the vial were mixed using a shaker (IKA; mechanical laboratory shaker: MS 3 basic). Sediment for pore water chemistry was collected from the interval shown in Table 3.3-3 using a spatula, and put into an outer pipe (Fig. 3.3-8). The surface sediment was scraped off to prevent from any contamination, and the sediment adherent to the PVC pipe was not sub-sampled due to the same reason.

2-2) Multiple corer

First, the water above the sediment in the multiple corers was collected with a syringe and filtered by a filter (ADVANTEC; DISPOSABLE SYRINGE FILTER UNIT 0.45 μm) before being placed in a 4 mL high density polyethylene narrow mouth bottle (NALGENE). The sediment was then cut out and collected every 5 cm using a push rod. The sediment adherent to the inner pipe was removed because it may have been contaminated with seawater. For each 5 cm, 5 cm^3 of sediment was collected from the surface for moisture content measurement and headspace gas analysis. These sampling procedures were the same as for the sediment sub-sampling from the piston corer.

2-3) Deep seawater

Deep seawater was sampled by a Niskin water sampler (General Oceanics), and sub-sampled from the sampler to a 20 mL syringe with a filter (ADVANTEC; DISPOSABLE SYRINGE FILTER UNIT 0.45 μm). The filtered deep seawater was distributed into two 4 mL high density polyethylene narrow mouth bottles (NALGENE). The samples in the bottles were stored in the refrigerator until their analyses.

2-4) Pore water squeezing

The collected sediment was put into the outer pipe preset with filter paper (Advantec; FILTER PAPER No. 2) and metal mesh (Kyuho Metal Corporation; 30 mesh: E9107) as shown in Fig. 3.3-8. A cylinder piston was put on the sediment sample in the outer pipe, and was pressed by a hydraulic press set (Fig. 3.3-9) consisting of a pump (RIKEN; SMP-3012B), a press frame (RIKENTable; CDM type press frame: CDM-10M), and a cylinder (RIKEN; single-acting cylinder: MS05-100) with a pressure of 10 MPa, and the sediment was squeezed to extract pore water into a syringe (HENKE; luer tip all plastic syringe) through a pore water extraction port (Fig. 3.3-9). The squeezed sediment was put into a plastic bag with zipper and stored in the freezer. The pore water collected in the syringe was filtered through a filtration filter (ADVANTEC; DISPOSABLE SYRINGE FILTER UNIT 0.45 μm) into two 4 mL high density polyethylene narrow mouth bottles (NALGENE) and stored in the refrigerator and freezer, respectively.

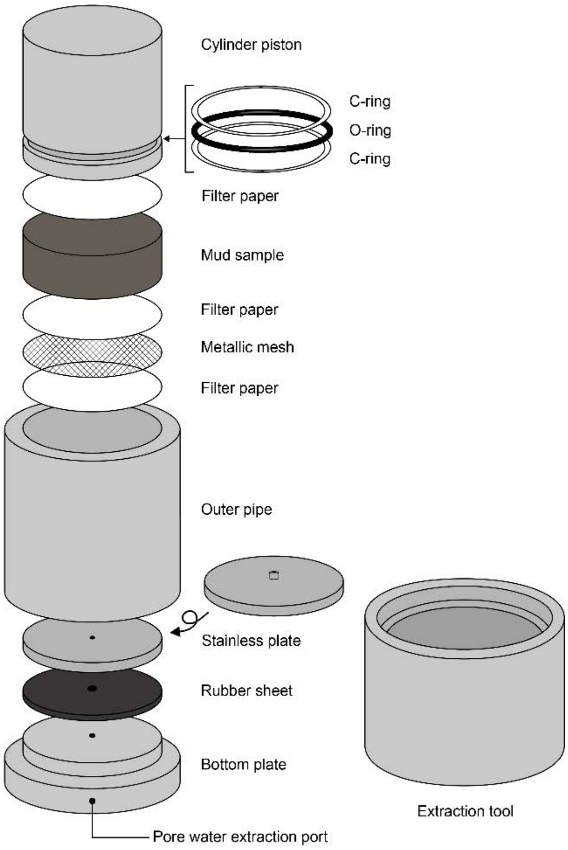

Figure 3.3-8. Assembly diagram of the cylinder for pore water extraction.

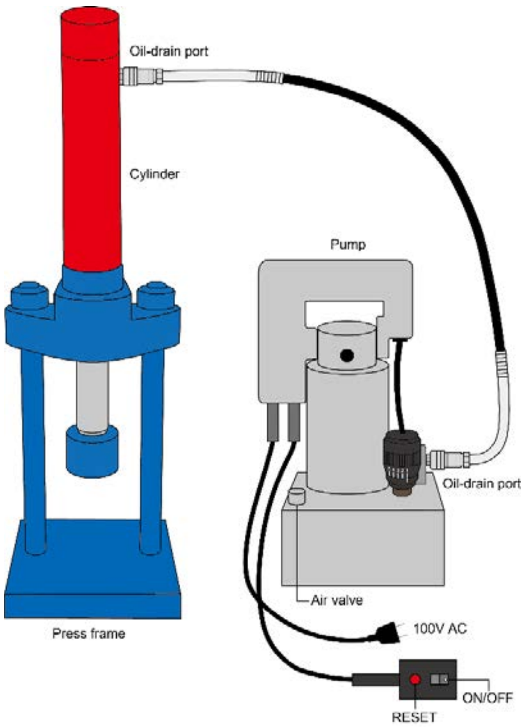

Figure 3.3-9. Schematic diagram of a hydraulic pump for pore water extraction.

3) Analytical methods

3-1) pH

To calibrate the pH, approximately 4 mL of pH 7 standard solution (Kanto Chemical Co., Ltd. neutral phosphate pH standard solution) was placed in a 10-cc bar bottle and a stirrer (ASONE; PASOLINA MINI STIRRER: CT-1A) was turned on. The pH 7 calibration was carried out by lowering the electrode so that the pH sensor (HORIBA; LAQUA: 9618S) was immersed in the solution, and the pH 7 calibration was performed by pressing START when the stability reached 0.001. The pH was then calibrated in the same way with a standard solution of pH 4 (Kanto Chemical Co., Ltd.; Phthalate pH Standard Solution), which was calibrated every measurement day. 2 mL of pore water and a magnetic rotator were placed in a 3.5 cc screw tube bottle (ASONE; NO.01), and then the pH meter was placed on a stirrer (HORIBA; pH meter; F-52).

3-2) Alkalinity

After measuring pH, 0.1 mol/L hydrochloric acid was added to the sample and the titration of hydrochloric acid when the electromotive force was between 220 and 240 mV was recorded. The gran factor (F) was obtained from the Eq. 1, and the intercept of the equation relating F to the amount of acid added was obtained. The alkalinity of IAPSO was determined using practice seawater on each measurement day when the samples were measured, and the alkalinity of IAPSO was measured after ensuring that the precision of the last three measurements was within 5%; the true value of the alkalinity of IAPSO was set to 2.45 and the difference between the measured values was used to correct the alkalinity value of the pore water samples. The error of measurement (maximum) was 3.5% in this cruise.

$$F = (v + V_0)\times10^{(E / 59.16)} \qquad \text{Eq. 1}$$

$$A_T = V_2N \cdot 1000 / V_0 \qquad \text{Eq. 2}$$

v : acid drop volume (cm^3)

V_0 : Initial volume of sample (cm^3)

E : Electromotive force of the pH electrode (mV)

A_T : Alkalinity (mM)

V_2 : Amount of acid added to the equivalent point

N : Prescribed degree of hydrochloric acid

3-3) Alkalinity

A few drops of filtered (ADVANTEC; DISPOSABLE SYRINGE FILTER UNIT 0.45 μm) sample were placed on a hand-held refractometer (Atago: IS/Mill-E), and the scale was read while the cover was placed on the instrument and pointed at a bright spot. Before measuring the sample, the sample was zeroed with ultrapure water.

Table 3.3-3. Depth of sediment sub-sampled to extract pore water and volume of pore water obtained

Core	Section	Length cm	Interval cm	Depth cmbsf	Volume mL	Remarks
MC01 DSW				−100		
HFPC01	2	81	15 − 25	20	30	
			50 − 60	55	30	
	3	100	20 − 30	106	30	
			70 − 80	156	30	
	4	100	60 − 80	247	30	void：26 − 30 cm
MC02 DSW				−100		
MC02	0		−30 − 0	−30		
	1		0 − 5	3	60	
	2		5 − 10	8	60	
	3		10 − 15	13	60	
	4		15 − 20	18	60	
	5		20 − 24	22	30	
MC03 DSW				−100		
HFPC03	2	115	15 − 25	40	40	
			75 − 85	86	45	void：40 − 54 cm
	3	28	10 − 20	136	40	
	4	64	10 − 20	164	50	
			40 − 50	194	30	

3.3.5. Interstitial water geochemistry (3) volatile elements

1) Background and purpose

Geochemical characteristics and behavior of pore fluids may be strongly related to tectonic settings and physical phenomena at convergent plate boundaries such as fault-bending and great earthquakes. Isotopic compositions of volatile elements in pore fluids provide crucial information reflecting fluid origins and cycles. For example, helium-3 is one of the most useful tracers for fluid behavior because of its chemical inertness and high sensitivity of mantle-derived components. In this study, isotopic compositions of volatile elements such as noble gases in porewater will be analyzed in order to investigate origins and cycles of fluids around faults which may affect subduction processes as fluid pathways between ocean and the interior of the Earth.

2) Sediment and seawater sampling

Sediment and seawater samples were collected at stations MC01, MC02 and MC03.

3) Methods

Sediment samples were collected using the multiple-corer system (MC). The liner made of acrylic (60-cm long) with through holes on the wall was used for sampling. The holes were sealed during core recovering. After core arriving on the deck, copper tubes were connected to the holes in order to transfer sediment into the tubes by squeezing using a jack. Immediately after squeezing, both ends of the copper tubes were sealed by metal clamps in order to avoid air contamination. Seawater samples were collected using a Niskin water sampling bottle mounted on the metal frame of MC. The bottle was equipped with a triggering system using a weight which closes the bottle at two meters above the seafloor. On land, porewater will be extracted from the sediment by centrifugation, and dissolved gases will be extracted from porewater and seawater samples. After purification of the gases, chemical and isotopic compositions of volatiles such as noble gases will be measured.

4) Results obtained just after the cruise

Isotopic compositions of helium and neon in some samples were measured at Atmosphere and Ocean Research Institute, The University of Tokyo in September 2020. Porewater was extracted from the sediment by centrifugation. Then gases dissolved in the pore fluid and seawater samples were extracted and introduced into the vacuum line connected to a QMS and a noble gas mass spectrometer (Helix SFT). In the line, the sample gases were purified and $^{4}He/^{20}Ne$ ratios were measured with the QMS, and $^{3}He/^{4}He$ ratios were measured with Helix SFT. The obtained isotopic ratios were calibrated against those of the atmosphere standard.

$^{3}He/^{4}He$ and $^{4}He/^{20}Ne$ ratios in porewater were basically higher than those of seawater and showed increasing trends with depths. This may indicate that there are fluid sources affected by mantle components in deeper layers around stations MC01, MC02 and MC03. In the KS-19-14 cruise by R/V Shinsei-Maru, porewater samples were collected at stations KS-19-14-PC07 and PC09 which were respectively close to stations KH-20-8-MC01 and MC03. KS-19-14 samples also had high $^{3}He/^{4}He$ and $^{4}He/^{20}Ne$ ratios, which is consistent with the data obtained in this study.

3.3.6. Marine magnetotelluric survey

1) Background and objectives

Fracture development process in the incoming oceanic plate can be examined through electromagnetic surveys, which reveal the electrical resistivity structure reflecting the distribution and connectivity of pore fluid. We have been conducting marine magnetotelluric (MT) surveys and controlled-source surveys on the outer rise of the Japan Trench. Analysis of MT data around 39.5°N indicated that the resistivity of the uppermost part of the Pacific plate varies with the distance from the trench. For further investigation of this feature, we deployed four ocean bottom magnetometers (OBEMs) in July 2019 on the KS-19-13 cruise of the R/V SHINSEI MARU. On this cruise we recover the four OBEMs. Analysis of the obtained data together with the existing data will reveal more detailed resistivity structure of the incoming Pacific plate, which would allow us to better estimate water distribution and temperature structure in the upper part of the subducting slab.

2) Instruments (OBEM)

The OBEM system can measure time variations of three components of magnetic field, two components of horizontal electric field, instrumental tilts, and temperature. We used two types of OBEM systems with the arm holding system (Japan Patent no. 4346605). One is the original type (Kasaya and Goto, 2009), which mainly consists of one 17-inch glass sphere, sensor unit in titanium pressure housing and electrode arm unit (Fig. 3.3-10 (a)). The glass sphere contains a data logger with 8 Hz sampling rate and a lithium battery pack. The sensor unit has a high-accuracy fluxgate magnetometer, tiltmeter and thermometer. The other is new type OBEM with 20 Hz sampling rate, and the fluxgate magnetometer unit was improved with highly sensitive sensor in short-period band and the electrometer was improved with ultra-low noise circuits (Fig. 3.3-10 (b)). The electrodes are Ag-AgCl equilibrium type made by Clover tech Inc. Four voltage differences between the electrodes on the tip of the pipes and the ground electrode are measured. A transponder unit, a radio beacon and a flashlight are also mounted on each OBEM. The acoustic system can communicate with the SSBL system of the ship and it is easy for us to detect its position in the sea or on the seafloor. The battery life of the acoustic system is two years.

3) Recovery of OBEMs

We retrieved four OBEMs at the sites N-G, N-H, N-I and N-J. We sent the acoustic weight-release signal through the SSBL system of the R/V HAKUHO MARU. The OBEMs were found with eyes and radio beacon signal soon after the surfacing. Arms of the OBEMs are folded when the OBEM is floating for easy recovery by the ship. The OBEMs were hooked and lifted up onto the deck on the starboard side. Conditions of the OBEMs were checked after removing the arm-unit, sensor unit and transponder. Then the glass-spheres were opened to check condition of the inside, to compare the OBEM clock with NTP clocks and, to read out the data. High quality time series data were obtained at all the sites.

(a) (b)

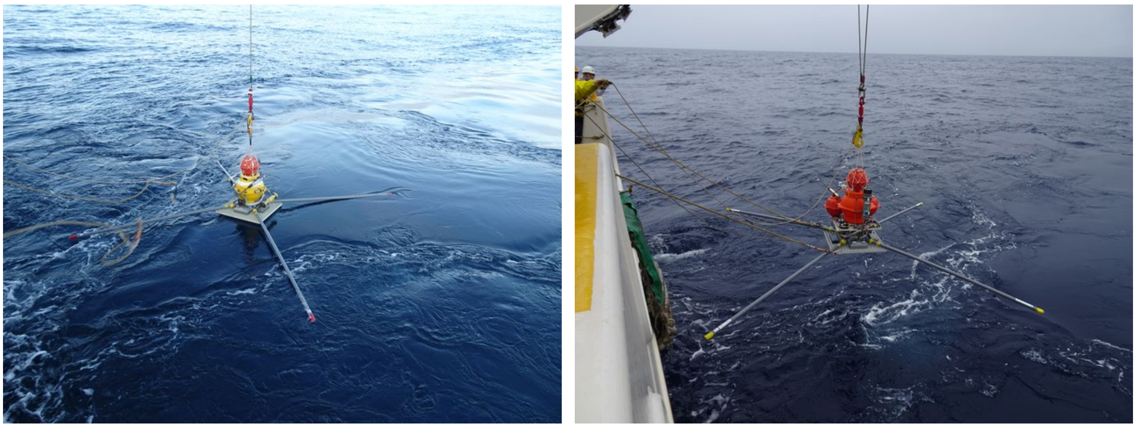

Figure 3.3-10. (a) Original type OBEM (KYT100). (b) New OBEM system with highly sensitive fluxgate magnetometer.

Table 3.3-4. Information on recovered OBEMs

Station	OBEM ID	Deployment	Recovery	Coordinates		Water depth (m)
N-G	JM402	Jul. 17, 2019	Aug. 26, 2020	39-27.04 N	144-47.64 E	5810
N-H	JM406	Jul. 17, 2019	Aug. 25, 2020	39-24.48 N	145-04.41 E	5480
N-I	JM401	Jul. 17, 2019	Aug. 25, 2020	39-21.81 N	145-22.38 E	5320
N-J	KYT100	Jul. 18, 2019	Aug. 25, 2020	39-18.19 N	145-44.68 E	5290

3.3.7. Activities in the Sagami Bay area

1) Background and objectives

Great earthquakes repeatedly occurred along the Sagami Trough where the Philippine Sea Plate subducts beneath the Okhotsk Plate, and devastated Tokyo and surrounding areas in 1923. A plate boundary fault was imaged by onshore-offshore integrated seismic survey campaigns. The splay fault was also recognized at the base of the eastern slope of the Sagami Bay. However, shallow sediment deformations by recent historical earthquakes have not been clarified. We conducted deep towed Subbottom profile (SBP) survey and pinpoint sediment sampling by the remotely operated vehicle NSS during the HAKUHO MARU cruises KH-10-3, KH-15-2 and KH-16-5. SBPs in the landward trench slope show landward reflectors reaching the seafloor surface. We also deployed one pop-up heat flow instrument (PHF) for long-term monitoring of vertical temperature distribution in surface sediment at a seep site characterized by chemosynthetic biological colonies during KH-19-5 cruise. The purpose of our study is to take sediment cores for determination of depositional ages and to retrieve the PHF for investigation of seep activity.

2) Results

One multiple core and one piston core operation were conducted in this cruise. The multiple core MC04 is located 900 m away from the fault-scarp base of the Miura Knoll (Fig. 3.3-11). Appearance through the coring tube shows dark olive structureless mud. The piston core PC04 is located at the fault-scarp base of the Miura Knoll. The total core length is 2.9 m. A pilot core (45 cm) is also obtained by a short gravity corer.

We failed to retrieve the PHF. The instrument answered to acoustic calls from the ship and accepted a command for releasing the weight, but the release unit did not work properly. The release command was sent repeatedly but not successful. We will try to recover the PHF with some other method.

We also conducted bathymetry mapping with a multi-beam echo-sounder and surface sediment structure survey with a sub-bottom profiler around the core sampling stations. The surveyed lines are summarized in Tables 3.3-5.

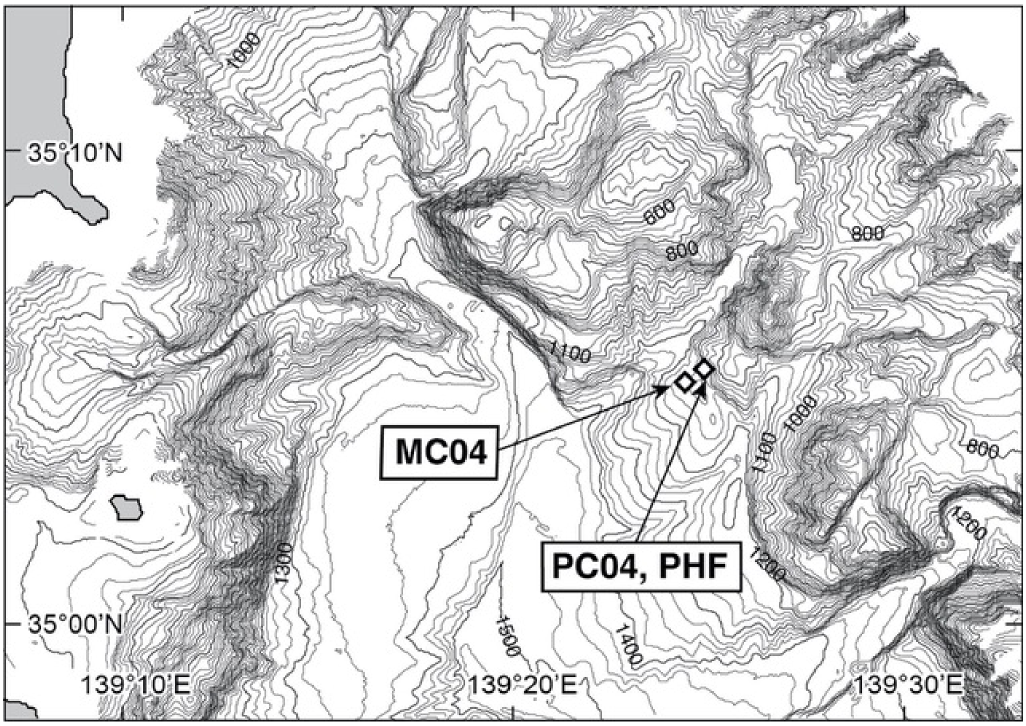

Figure 3.3-11. Bathymetric map of the central Sagami Bay. Our survey site is located at the fault-scarp base of the Miura Knoll.

Table 3.3-5. Bathymetry and sub-bottom profiling survey lines in the Sagami Bay area

No.	End point 1		End point 2	
	Latitude (N)	Longitude (E)	Latitude (N)	Longitude (E)
Line A	35°07.375'	139°24.644'	35°05.346'	139°22.168'
Line B	35°07.022'	139°25.075'	35°04.992'	139°22.599'
Line C	35°06.668'	139°25.507'	35°04.639'	139°23.030'
Line D	35°06.315'	139°25.938'	35°04.285'	139°23.462'
Line E	35°05.961'	139°26.370'	35°03.932'	139°23.893'
Line F	35°05.608'	139°26.801'	35°03.578'	139°24.325'
Line G	35°05.254'	139°27.232'	35°03.225'	139°24.756'

3.3.8. Aerosol and surface water sampling

1) Research objectives

To accurately assess the origin and composition of seafloor sediments and stromal waters, it is necessary to distinguish between atmospheric dry deposition, advection from coastal, and landslides. Seafloor sediments are composed of atmospheric dry deposition, as well as inflows from the coast, horizontal advection from other waters, and biological activity by living organisms. In orders to understand the contribution of each source to the composition of sea floor sediments, we observed the atmospheric dry deposition in addition to direct sampling and measurement of the sea floor sampling. We believe this make it possible to define the characteristics of the Kuril Trench and its surrounding environment from the viewpoint of material transportation.

In this cruise we have collected aerosol samples to understand the effects of atmospheric deposition on seafloor sediments. We also have collected samples for Chl-a, Cells Counting, Biomarker that are useful in assessing the contribution of aerosol to surface ocean primary production and the impact of primary production on seafloor sediments.

2) Sampling methods

Aerosol:

The high-volume air sampler (KIMOTO 120SL) and the Andersen air sampler (Tokyo Direc Corporation AN-200) were installed on the upper deck. The wind vane and anemometer were installed with the air sampler to avoid contamination from the ship’s exhaust; limited power was turned on when the headwind (120 deg; -60 to +60 deg relative to the bow) and with the wind speed greater than 3 m/s. The detailed sampling area is shown in Fig. 3.3-12 and Table 3.3-6.

Chl-a, Cells Counting, Biomarker:

The samples were collected from the surface ocean (0 m, underway) with the pumping system. About 250 ml of sea water was collected for Chl-a samples with GF/F and membrane filter (pore size; 10 μm, 5 μm, 2 μm). About 500 ml of sea water for collected for Cells Counting with 0.45 μm membrane filters. About 180 L of sea water was collected for Biomarker with GF/F filter.

REEs:

Rare Earth Elements samples were collected from the surface ocean (0m, underway) by the pumping system. About 500 ml of sea water for REEs with 0.2 μm membrane filters. After filtration, hydrochloric acid was added to prevent the denaturation of the components.

The detailed locations where Chl-a, Cell Count, Biomarker, and REEs samples were collected are shown in Table 3.3-7.

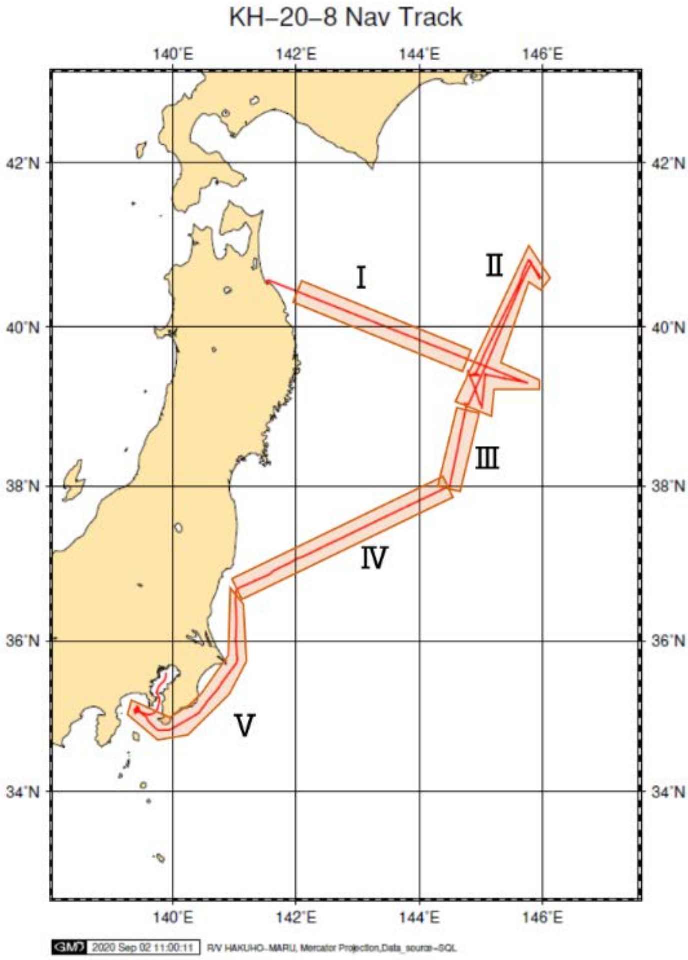

Figure 3.3-12. Aerosol sampling area.

Table 3.3-6. Aerosol sampling locations

Sample Area	Start/Finish	Date(JST)			Time(JST)	Position					
I	Start	2020	08	24	16:16	40	25.9076	N	142	02.3152	E
	Finish	2020	08	27	6:00	39	24.9530	N	144	53.7820	E
II	Start	2020	08	27	13:55	39	25.2144	N	144	55.1233	E
	Finish	2020	08	29	17:15	39	02.08	N	144	46.22	E
III	Start	2020	08	29	17:15	39	02.08	N	144	46.22	E
	Finish	2020	08	30	17:12	37	59.5117	N	144	29.3769	E
IV	Start	2020	08	30	17:12	37	59.5117	N	144	29.3769	E
	Finish	2020	08	31	7:59	36	47.0231	N	141	20.0025	E
V	Start	2020	08	31	8:26	36	43.4899	N	141	11.1421	E
	Finish	2020	09	01	16:21	35	05.58	N	139	44.79	E

Table 3.3-7. Chl-a, Cells Counting, Biomarker, REEs sampling locations

Sampling No.	Method	Date(JST)			Time(JST)	Position					
S0-1	pump	2020	08	24	17:02	40	21.9406	N	142	13.1814	E
S0-2	pump	2020	08	24	20:19	40	12.4417	N	143	12.4417	E
S0-3	pump	2020	08	24	22:58	39	50.2328	N	144	00.0001	E
S0-4	pump	2020	08	25	6:37	39	18.3290	N	145	44.7235	E
S0-5	pump	2020	08	25	11:00	39	21.7038	N	145	22.2654	E
S0-6	pump	2020	08	25	14:16	39	24.6057	N	145	04.1690	E
S0-7	pump	2020	08	25	19:20	38	59.4505	N	145	00.7361	E
S0-8	pump	2020	08	26	10:55	39	27.0271	N	144	47.4857	E
SS-8	bucket	2020	08	26	13:00	39	27.1890	N	144	47.5394	E
S0-9	pump	2020	08	27	14:30	39	33.4902	N	145	00.0190	E
S0-10	pump	2020	08	27	16:28	40	00.0120	N	145	16.4972	E
S0-11	pump	2020	08	27	17:35	40	15.0102	N	145	26.2328	E
S0-12	pump	2020	08	27	18:53	40	32.2059	N	145	37.4420	E
S0-13	pump	2020	08	28	9:32	40	36.9561	N	145	58.0259	E
S0-14	pump	2020	08	28	16:33	40	47.7820	N	145	48.6639	E
SS-14	bucket	2020	08	28	17:00	40	47.7820	N	145	48.6639	E
S0-15	pump	2020	08	29	0:53	40	21.2756	N	145	33.2520	E
S0-16	pump	2020	08	29	2:53	39	54.4300	N	145	18.1524	E
S0-17	pump	2020	08	29	4:56	39	28.7555	N	145	03.4931	E
S0-18	pump	2020	08	29	12:28	39	01.9488	N	144	45.6659	E
SS-18	bucket	2020	08	29	13:00	39	01.9488	N	144	45.6659	E
S0-19	pump	2020	08	30	0:39	38	44.0286	N	144	41.3278	E
S0-20	pump	2020	08	30	1:42	38	29.3094	N	144	37.6163	E
S0-21	pump	2020	08	30	2:45	38	14.4432	N	144	33.5515	E
S0-22	pump	2020	08	30	12:15	37	59.9000	N	144	29.7169	E
SS-22	bucket	2020	08	30	12:37	37	59.9000	N	144	29.7169	E
S0-23	pump	2020	08	30	22:55	37	44.0506	N	143	47.2469	E
S0-24	pump	2020	08	31	1:23	37	28.3137	N	143	05.7328	E
S0-25	pump	2020	08	31	4:00	37	12.4816	N	142	24.3793	E
S0-26	pump	2020	08	31	6:33	36	56.7103	N	141	43.1610	E
S0-27	pump	2020	08	31	8:59	36	40.1525	N	141	01.8963	E
S0-28	pump	2020	08	31	11:20	36	04.9928	N	141	01.4426	E
S0-29	pump	2020	08	31	12:54	35	42.3682	N	141	01.8895	E
S0-30	pump	2020	08	31	14:31	35	22.3164	N	140	43.9819	E
S0-31	pump	2020	08	31	16:01	35	04.8242	N	140	26.8783	E
S0-32	pump	2020	08	31	17:02	34	56.7244	N	140	11.9597	E
S0-33	pump	2020	08	31	17:53	34	50.2915	N	139	58.6475	E
S0-34	pump	2020	08	31	18:31	34	49.2904	N	139	47.6819	E
S0-35	pump	2020	08	31	19:35	34	56.8220	N	139	35.8485	E
S0-36	pump	2020	09	01	8:29	35	05.4055	N	139	24.8703	E
SS-36	bucket	2020	09	01	8:10	35	05.4055	N	139	24.8703	E

3) Anticipated results and future work plans

After disembarking from the cruise, the major components of the aerosol samples will be analyzed with ion chromatography, and REEs (both the aerosol samples and water samples) will be measured with ICP-MS (ELEMENT-II) using the isotope dilution method at the University of Toyama. The data will be analyzed and their influence on the surface ocean and seafloor sediment will be analyzed.

Chlorophyll-a will be measured by a Tuner Design Fluorometer, and the Cells Counting samples will be analyzed with a Scanning Electron Microscope at the University of Toyama. Biomarker samples will be measured at the Ocean University of China.

The samples analyses are expected to be finished within one year after the cruise and the results will be submitted by middle 2022.

4. References

Bristow, K.L., G.J. Kluitenberg, and R. Horton (1994) Measurement of soil thermal properties with a dual-probe heat-pulse technique, *Soil Sci. Soc. Am. J.*, **58**, 1288-1294.

Deyhle, A. and A.J. Kopf (2005) The use and usefulness of boron isotopes in natural silicate–water systems, *Phys. Chem. Earth, Parts A/B/C*, **30,** 1038-1046.

Kasaya, T. and T, Goto (2009) A small ocean bottom electromagnetometer and ocean bottom electrometer system with an arm-folding mechanism (Technical Report), *Exploration Geophysics*, **40**, 41-48; *Butsuri-Tansa*, **62**, 41-48; *Mulli-Tamsa*, **12**, 41-48.

Kawada, Y., M. Yamano, and N. Seama (2014) Hydrothermal heat mining in an incoming oceanic plate due to aquifer thickening: Explaining the high heat flow anomaly observed around the Japan Trench, *Geochem. Geophys. Geosyst.*, **15**, 1580–1599, doi:10.1002/2014GC005285.

Park, J.-O., N. Takahata, E. Jamali Hondori, A. Yamaguchi, T. Kagoshima, T. Tsuru, G. Fujie, Y. Sun, J. Ashi, M. Yamano, Y. Sano (2021) Mantle-derived helium released through the Japan trench bend-faults, *Sci. Rep.*, **11**, 12026, doi:10.1038/s41598-021-91523-6.

Sass, J.H., C. Stone, and R.J. Munroe (1984) Thermal conductivity determinations on solid rocks - a comparison between a steady-state divided-bar apparatus and a commercial transient line-source device, *J. Volcanol. Geotherm. Res.*, **20**, 145-153.

Spivack, A.J., M.R. Palmer, and J.M. Edmond (1987) The sedimentary cycle of the boron isotopes, *Geochim. Cosmochim. Acta*, **51**, 1939-1949.

Williams, L.B., R.L. Hervig, J.R. Holloway, and I. Hutcheon (2001) Boron isotope geochemistry during diagenesis. Part I. Experimental determination of fractionation during illitization of smectite, *Geochim. Cosmochim. Acta*, **65**, 1769-1782.

Yamano, M., H. Hamamoto, Y. Kawada, and S. Goto (2014) Heat flow anomaly on the seaward side of the Japan Trench associated with deformation of the incoming Pacific plate, *Earth Planet. Sci. Lett.*, **407**, 196-204.

You, C.F., P.R. Castillo, J.M. Gieskes, L.H. Chan, and A.J. Spivack (1996) Trace element behavior in hydrothermal experiments: Implications for fluid processes at shallow depths in subduction zones, *Earth Planet. Sci. Lett.*, **140**, 41-52.

You, C.F., A.J. Spivack, J.M. Gieskes, R. Rosenbauer, and J.L. Bischoff (1995) Experimental study of boron geochemistry: implications for fluid processes in subduction zones, *Geochim. Cosmochim. Acta*, **59**, 2435-2442.

Von Herzen, R. and A.E. Maxwell (1959) The measurement of thermal conductivity of deep-sea sediments by a needle-probe method, *J. Geophys. Res.*, **64**, 1557-1563.

5. Notice on Using

This cruise report is a preliminary documentation as of the end of cruise.
This report is not necessarily corrected even if there is any inaccurate description (i.e. taxonomic classifications). This report is subject to be revised without notice. Some data on this report may be raw or unprocessed. If you are going to use or refer the data on this report, it is recommended to ask the Chief Scientist for latest status.
Users of information on this report are requested to submit Publication Report to Cooperative Research Cruise office.

E-mail: kyodoriyo@aori.u-tokyo.ac.jp